Building and Environment 244 (2023) 110704

Contents lists available at ScienceDirect

Building and Environment

journal homepage: www.elsevier.com/locate/buildenv

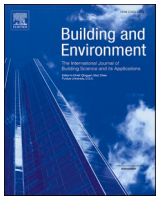

Increasing solar panel output with blue-green roofs in water-circular and nature inclusive urban development

Els van der Roest [a,b,*], Joris G.W.F. Voeten [c], Dirk Gijsbert Cirkel [a]

[a] KWR Water Research Institute, Groningenhaven 7, 3430 BB, Nieuwegein, the Netherlands
[b] Faculty of Civil Engineering and Geosciences, Delft University of Technology, Stevinweg 1, 2638 CN, Delft, the Netherlands
[c] Team Climate Resilience, Wageningen Environmental Research, P.O. Box 47, 6700 AA, Wageningen, the Netherlands

ARTICLE INFO

Keywords:
Blue-green roofs
Photovoltaic (PV)- green roof
Energy output
Grey water recycling
Constructed wetroof
Evapotranspiration

ABSTRACT

With an increasing demand for climate resiliency, water sensitivity, nature inclusiveness and energy efficiency in dense urban environments, the call for layered and multifunctional use of rooftops is rising. Vegetated roofs combined with Photo-Voltaic (PV) installations are an example of multifunctional and more effective use of available space, and well-irrigated systems could have an enhanced cooling effect. This research investigated a blue-green capillary irrigated solar roof with grey (shower-) water suppletion, with a constructed wetroof for grey water purification. Two full-scale commercial PV systems on twin rental apartment blocks in Amsterdam were analyzed, on a blue-green roof (BGR) versus a bitumen roof (BiR). The energy output, PV panel temperature, relative humidity and air temperature under the panels were monitored during 5 warmer months (June–October 2022). On average, a solar panel on the BGR is expected to produce 4.4% more energy than a solar panel on the BiR at similar irradiation. A clear difference in panel temperature on the roofs is only seen when the surface temperature of the roofs differs by at least 4.64 °C. Otherwise, other factors such as wind or albedo have probably more influence on the PV panel temperature and thus on PV power output.

1. Introduction

Expectations of multifunctionality and functional-layered urban design are rising. Urban environments need to reduce air pollution, adapt to climate change-induced drought, flooding and heat stress, and play a key role in the energy transition. At the same time, urban space is often scarce, and choices have to be made on how to utilize space effectively. Roofs are in general seen as an ideal location for local renewable energy production and on new buildings, PV panels are becoming indispensable to meet energy performance requirements. At the same time, greening roofs is seen as a promising solution for urban heat island mitigation, and stormwater runoff reduction [1,2] as well as reducing energy consumption for cooling, noise- and air pollution, while enhancing biodiversity [3,4]. Would this mean that we have to choose between energy production or the beneficial effects of vegetated roofs?

It is well known that the performance of PV modules decreases with increasing panel temperature, with a temperature coefficient of 0.2–0.4%/°C depending on the type of solar cell [5]. Moreover, there is a clear correlation found between the average daily air temperature under the PV module and the temperature of PV modules [6,7]. With these facts in mind, it has been shown that green roofs and PV are not necessarily in conflict over the same space, but can be combined on the same surface with possible positive effects for the energy production of solar panels.

Green roofs namely have transpiring plants that cool the air in their surroundings by shifting the distribution of energy from warming up air (sensible heat, H in J m^{-2}) to using energy for the evaporation of water (latent heat, LE in J m^{-2}). If water is abundantly available, LE on green roofs can become as high as 95% of net incoming radiation, R_n (J m^{-2}) on a long-term annual basis [2]. On a green roof, the evapotranspiration of the plants can thus lead to cooling of the air under the panels, which in turn positively affects the PV efficiency [8,9]. As mentioned, water availability is crucial for evapotranspiration. When water becomes scarce, rooftop plants stop transpiring and the ratio H/LE can change from below 0.1 to more than 10 [2] resulting in strong heating of air. In this respect, so-called blue-green roofs are an interesting option. These roof systems capture and store rainwater under the vegetation layer, reducing stormwater runoff [10] and provide the vegetation with water, ideally through sub-surface capillary irrigation, for longer periods of time [2,11]. It is interesting to note that Schindler et al. (2018) [12] suggested that regular irrigation of green roofs in Mediterranean

* Corresponding author. KWR Water Research Institute, Groningenhaven 7, 3430 BB, Nieuwegein, the Netherlands.
E-mail addresses: els.van.der.roest@kwrwater.nl, e.vanderroest@tudelft.nl (E. van der Roest).

https://doi.org/10.1016/j.buildenv.2023.110704
Received 9 May 2023; Received in revised form 19 July 2023; Accepted 3 August 2023
Available online 6 August 2023

Nomenclature

BiR	Bitumen roof
BGR	Blue-green roof
H	sensible heat (J m^{-2})
h_{c-}	convective heat transfer coefficient (W $m^{-2}K^{-1}$)
kWp	kilowattpeak
LE	latent heat (J m^{-2})
η_{mp}	the efficiency of a solar cell (%)
$\eta_{mp,STC}$	Efficiency of a solar cell at standard test conditions (%)
α_P	Solar cell temperature coefficient of power (%/°C)
RH	Relative humidity (%)
P	precipitation (mm)
PV	photovoltaic
Q_H	sensible heat flux (W m^{-2})
R_n	net radiation (J m^{-2})
R_s	incoming short wave radiation (J m^{-2})
Irr	Irradiance (W m^{-2})
T_{amb}	Ambient air temperature (°C)
T_a	Air temperature underneath the solar panel (°C)
T_c	Cell temperature (°C)
T_P	Back of panel temperature (°C)
T_S	Roof surface temperature (°C)
v	Wind velocity (ms^{-1})
W	Watt (J/s)

climates could enhance the power output of PV-green roofs, and El Helow found water stress of the plants in Toronto causing them to evaporate less [13]. Osma-Pinto & Ordóñez-Plata [14] state that a green roof will only give a thermal benefit as long as it has a satisfactory moisture level (in tropical climates).

Although still limited, the number of studies quantifying the effect of green roofs on energy production of solar panels is increasing and the results so far are summarized in Table 1. The available studies show a positive effect of green (non-irrigated) roofs on PV performance with between 0.5 and 6% increase in power output (see Table 1). Yet, many studies have a small set-up [8,12,14–16] of only one or a few panels. Moreover, the set-ups of PV systems on green and bitumen/black roofs are often not comparable in height [12,14,17–19], although the height is indicated as a factor that influences solar panel performance [20,21]. Therefore, there is a need for more large-scale systematic research on green roofs with PV systems whereby the height of the panels above the roof is comparable between set-ups [20,21]. Also, the application of a blue-green roof could lead to continuous evapotranspiration of the vegetation during dry (and warm) periods and thus positively affect the PV panel efficiency. Therefore, our research question is:

Is there an increased performance of solar PV above a capillary irrigated, blue-green roof vs a bitumen roof in a temperate maritime climate?

To answer this question, research is performed on two identical rental apartment buildings in Amsterdam (The Netherlands), providing a unique setting for a large scale field study. The novel system set-up combines a blue-green roof with PV, and has additional water supply by transforming grey water from showers to irrigation water with a shallow rooftop version of a horizontal flow constructed wetland, a so-called constructed wetroof [22]. This way we opt to demonstrate the win-win-win situation for future buildings, contributing to energy production, local water reuse, reduction of urban drought and increasing biodiversity while reducing heat stress and flooding as a result of heavy rainfall.

2. Material and methods

2.1. General experimental setup

PV panels were placed on the rooftops of two identical six-story, 34.4 m high apartment buildings in Amsterdam (latitude 52.35°N, longitude 4.84°E). One building was equipped with a blue-green roof (BGR) and the other with standard bitumen roofing (BiR) (Fig. 1). The climate of the research site is temperate maritime, with an average maximum day temperature of 22.5 °C in July, average global radiation of 393 MJ $cm^{-2}yr^{-1}$, average precipitation of 880 mm yr^{-1} and an average Makkink reference crop evapotranspiration [25] of 627 mm yr^{-1} (period 1992 until 2022, from weather station Schiphol, located 7 km from the research site). On the roof of the western building, we installed a blue-green roof equipped with a Permavoid 85s rainwater retention and capillary irrigation system [26] and a substrate layer of 6 cm (see Fig. 2). The maximum water storage level in the Permavoid units was set to 60 mm. An added advantage of the full field surface capillary irrigation system is the fact that water availability for plants underneath and in between the rows of panels is equal. Because ample water is crucial for plant transpiration and thereby for cooling, we provided an additional water supply by transforming grey water from showers in the building on the roof using a shallow rooftop version of a horizontal flow constructed wetland, a so-called constructed wetroof [22]. This way a local source of irrigation water is available for the vegetated roof, even during dry spells, reducing the sewer loading and the use of drinking water for irrigation. The constructed wetroof [22] was integrated into a waterproof-lined section (ca 30 m^2) of the substrate layer in the blue-green roof, to receive and treat grey water (shower only), coming from a collection, pre-treatment and pump tank in the basement of the building, with an overflow of the treated water into the Permavoid rainwater retention units underneath the substrate layer. Using the treated grey water, the water level in the water storage layer below the vegetation is kept at a minimum of 50 mm, ensuring a sufficient water supply for the vegetation [2]. The initial vegetation consisted of sedum mix blankets from the company Sempergreen. After placement of the sedum mix blankets, 26 plant species native to the Netherlands were sown on the blankets.

The installed Jinko 405 Wp PV panels (see Table 2 for specifications) are facing south (180°) and are fixed at a 20° angle and have a size of 1.03 × 1.86 m in landscape position. The total system capacity on each roof is 23.78 kWp (62 panels per roof) of which 6 panels per roof were chosen for more detailed monitoring (see Fig. 3 and next section). The panels for detailed monitoring were chosen such that the panels on the blue-green and bitumen roofs are as close together as possible, yet the panels closest to the roof edge are excluded from the study as they will be influenced more by i.e. wind effects and less by vegetation. A sunlight study (Fig. 3) has shown that due to adjacent tall buildings, the eastern roof (the black roof) receives quite a lot of shade in the morning hours in spring and autumn. In summer the effect is less pronounced, and in winter shade has a similar impact on both buildings. To be able to correct for shade effects, we installed a pyranometer on both roofs (see next section).

The lower side of the panels were positioned 32 cm above the surface, being either the soil surface or the rooftop surface on both roofs to make sure that the results from both roofs are not influenced by distance between the roof and the panel [20,21] (for details see Fig. 2). Rows are spaced at 73 cm between the high end of a panel in one row and the low end of the panel in the next row. The reduction in electric efficiency due to the warming up of the panels compared to the efficiency at standard test conditions can be calculated as follows:

$$\eta_{mp} = \eta_{mp,STC}\left[1 + \alpha_P\left(T_p - T_{p,STC}\right)\right] \quad \text{(Eq 1)}$$

Table 1
Literature overview of studies focusing on green roofs with PV.

Study	Measured parameters	Location	Measurement design	Minimum panel height above the roof	Angle	Measurement duration/period	Increase in PV power output
Alshayeb & Chang (2018) [6]	Under panel air temperature, roof surface temperature, relative humidity, PV panel temperature, PV output. Weatherstation; wind speed + direction, solar radiation, ambient temperature, relative humidity.	Kansas, USA	9 panels with black roof surface, 9 panels with green roof (sedum) surface.	20 cm	10°	One year	3.3–5.3% extra PV power output with warm weather. Year round 1.4%.
Schindler et al. (2018) [12]	Substrate temperature, air temperature in front of the panel and at under the panel, panel temperature, PV output.	Haifa, Israel	Experimental plots on 4 × 3.8 m wooden frames.	Black: 50 cm Green: 30 cm	20°	18 months	No difference measured
Osma-Pinto & Ordonez-plata (2019) [14]	Solar irradiation, air temperature, air velocity, DC, AC power.	Buramanga, Colombia	Green and black plots constructed on one roof.	25/50/75/100 cm Vegetation decreases space between panel/surface with ca. 20 cm	10°	13 tests lasting for at least one week	1–1.3%
Perez et al. (2012) [15]	Internal building temperature, near surface roof temperature, back-of-module temperature, PV output.	New York City, USA	Very small setup with miniature 'houses' (about 0.5 m high).	Unknown	45°	8 months (May–January)	2.42% for PV above a green roof vs. a gravel roof
Chemisana & Lamnatou (2014) [16]	Module temperature on panel, on the surface beneath the panel, in the surface and the air above panel, PV output.	Lleida, Spain	Tiny panels (36.5 × 19.5 cm) in wooden trays (0.9 × 1.30 m^2) on a gravel roof With *Sedum* and *Gazania*.	2 cm (because of very small panels).	33°	2 months (June–July)	1.29–3.33% increase in maximum power output on a green vs gravel roof.
Köhler et al. (2007) [17]	PV power output, infrared temperature measurements	Berlin, Germany	Many different designs.	Green: 50 cm Bitumen: 0 cm	8–30°	5 years	6% for panels above green roof compared to bitumen.
Nagengast et al. (2013) [18]	Panel temperature on panel, PV output. Solar irradiance, measured parallel to the PV panel. Weather station on the roof with wind speed, direction, solar radiation, rain, ambient temperature	Pittsburg, USA	Large roof with different solar setups. 60 PV panels on moss green roof, 90 PV panels on black roof.	Black roof: 13 cm Green roof: 51 cm	15°	One year	Max. 0.5%
Alameddine et al. (2021) [19]	Biodiversity, air quality, thermal insulation properties, Stormwater runoff, PV output.	Sydney, Australia	335 panels (395 Wp) on a green roof, North facing, 346 panels (320 Wp) on the bitumen roof, East-West facing)	Not mentioned	15° on green, 5° on bitumen	234 days (8 months)	2.48% increased hourly energy output on green roof vs black roof.
Ogaili (2015) [20]	Temperature of back surface of panel, heat flux, air temperature, and windspeed under panel, surface temperature, DC voltage, DC current, AC power.	Portland, USA	Roof with PV rack with 0.3 m distance between panels, both with white, black and green (*Dianthus*) surface. Sensors were placed at two panels at the same time and conditions (surface/height) were changed over time	18 cm and 24 cm above roof surface	30°	At least 3 sunny days per condition, experiments lasted from July to September.	At 18 cm: 1.2% PV-green roof vs black roof, 0.8% more above a PV-green roof vs white roof. At 24 cm: 1.0% PV-green roof vs. black roof, 0.7% for a PV-green roof vs. white roof.
Osma et al. (2016) [23]	PV output.	Bucaramanga, Colombia	3 panels installed on a green (sedum, 7 cm substrate) roof, vegetation could be removed under a panel to obtain a black surface (black)	50 cm and 75 cm above the roof surface	10°	3 weeks	Lower height increases PV output by 2%, a green roof increases the PV output by ca 1%.
El Helow (2017) [24]	Temperature of back surface of panel, PV output, biomass data, ambient temperature.	Toronto, Canada	40 panels on a white roof, in four rows with green beds (grasses and wildflower species) underneath at different heights.	61 cm and 122 cm above the roof surface	–	About 7 weeks	Larger height increases cooling effect. More biomass growth (18%) with higher distance. WR vs GR – 1.1% higher on GR. GR 122 cm 2.2% higher output than at 61 cm.

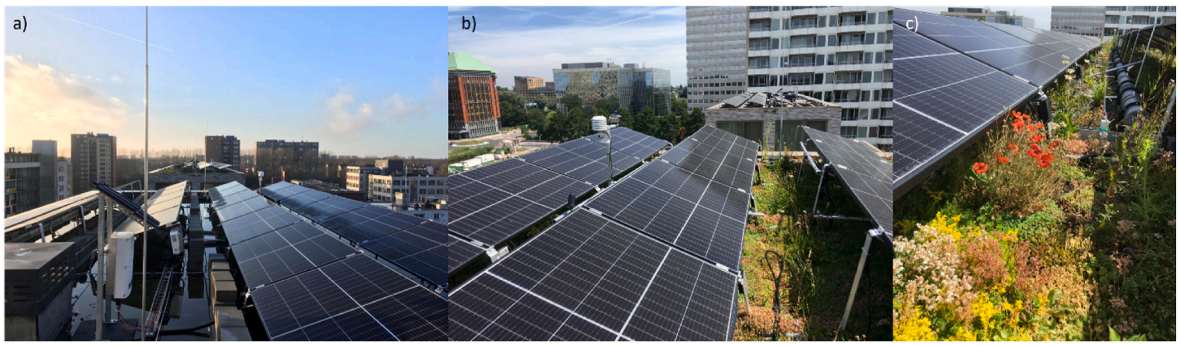

Fig. 1. Overview of (a) the BiR, (b) the BGR (c) the blooming BGR with the integrated constructed wetroof in the background (grey PVC water inlet distribution pipe).

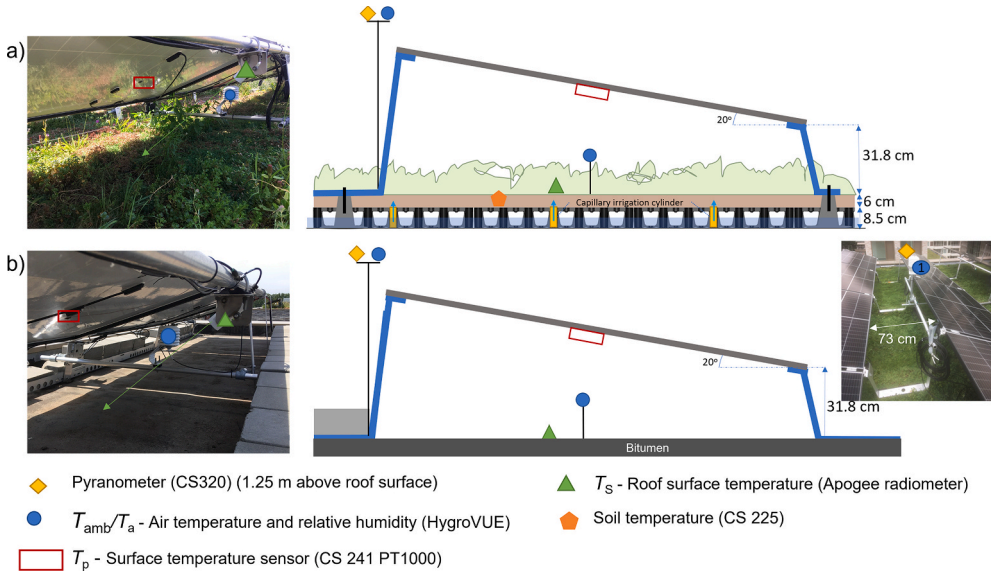

Fig. 2. Overview of sensor types and locations on the blue-green roof BGR (a) and bitumen roof BiR (b), including the design of the blue-green roof with capillary irrigation system below the substrate layer. The Apogee sensor is pointed towards the roof surface and thus measures the roof surface temperature below the panels. (For interpretation of the references to colour in this figure legend, the reader is referred to the Web version of this article.)

Table 2
PV panel characteristics of the Jinko Solar 405Wp panels.

Panel characteristic	Unit	Value
Maximum Power Output at STC	W	385
Module efficiency ($\eta_{mp,STC}$)	%	20.17
Nominal Operating Cell Temperature (NOCT)	°C	45 ± 2
Temperature coefficient of P_{max} (α_P)	%/°C	−0.35
Temperature coefficient of Voc	%/°C	−0.28
Temperature coefficient of Isc	%/°C	−0.048

With η_{mp} (%) the efficiency of the solar cell, $\eta_{mp,STC}$ the efficiency (%) at standard test conditions (STC), α_P the temperature coefficient of power (P_{max}) in %/°C, T_p the panel temperature and $T_{p,STC}$ the cell temperature at standard test conditions (25 °C). Characteristic values for $\eta_{mp,STC}$ and α_P are given in Table 2.

2.2. Data acquisition

On each roof, a section of six panels was equipped with sensors to measure incoming short wave radiation R_s (J m^{-2}), ambient air temperature T_{amb} (°C), air temperature below the PV panels T_a (°C), relative humidity *RH* (%), surface temperature T_s (°C), substrate temperature T_{sub} (°C) and back of panel temperature T_p (°C) (Fig. 2 & Table 3). Precipitation *P* (mm) was measured with a rain gauge (ARG314, EML Ltd.) on the blue-green roof. Incoming shortwave radiation (R_s) was measured at 1.25 m above the roof surface using pyranometers (CS320, Campbell Scientific Inc.). Air temperature (T_{amb} & T_a) and relative humidity (*RH*) were measured using a combined element (HygroVUE5, Campbell Scientific Inc.) placed in a radiation shield next to the pyranometer and below each pair of solar panels at a height of 40 cm. The surface temperature (T_s) of the vegetation and bitumen was measured, in the shade, below three panels on each roof using infrared radiometers (SI-431-SS, Apogee Instruments). The substrate temperature (T_{sub}) was measured at two locations below the panels on the blue-green roof using a temperature sensor string (CS225, Campbell Scientific Inc.). PV panel temperature (T_p) was measured at the back of each of the six panels on each roof using back-of-module temperature sensors (CS241, Campbell Scientific Inc.). Measurements were collected at 10 min intervals, aggregated to hourly values, and logged on a datalogger (CR380, Campbell Scientific Inc.). Wind data was obtained from the nearby Schiphol weather station. Besides the detailed measurements the energy output of each panel on the two roofs is logged on an hourly basis. The PV panels are installed with microinverters to avoid string effects, enabling us to measure PV output of each panel at hourly intervals via the SolarEdge data platform.

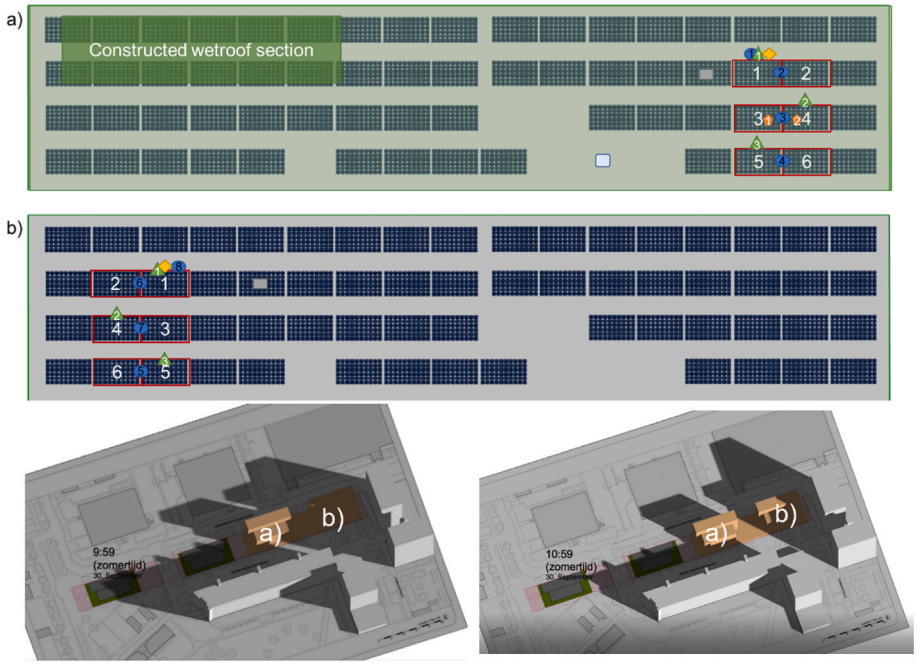

Fig. 3. Schematic overview of the chosen panels for monitoring on the western blue-green roof (a), and the eastern bitumen roof (b). The panels for detailed monitoring are chosen in such a way that the differences in shading are kept to a minimum. The symbols represent sensors and are explained in Fig. 2, the green block on the blue-green roof (a) represents the part of the roof that is designed as a constructed wetroof, the rest of the roof is sedum in combination with 26 native plant species. The shade situation is given for 30 September 9:59 (bitumen roof is still in the shade) and 10:59 (half of the bitumen roof is in the sun). (For interpretation of the references to colour in this figure legend, the reader is referred to the Web version of this article.)

Table 3
Overview of sensor type, characteristics and location. Sensor locations are shown in Fig. 2.

Sensor	Accuracy	Operating temperature	Amount	Location
HygroVUE5 air temperature and relative humidity (RH)	±0.3–0.4 °C ±1.8–3% (RH)	−40 °C–70 °C	3 per roof/1 per roof	Under panel/ 1.25 m above panel
CS320 pyranometer	±2.6%	−50 °C–60 °C	1 per roof	1.25 m above panel
Apogee radiometer SI-431-SS	±0.2 °C	−30 °C–65 °C	3 per roof	Mounted in the middle of the panel
CS 241 PT1000	±(0.15 + 0.002t)°C	−40 °C–150 °C	6 per roof	Placed on the back side of the panel (in the middle)
ARG314 Raingauge	99% up to 120 mm/h	+1 °C–70 °C	1 (on blue-green roof)	Open location on the roof
CS225 Temperature sensor	±0.2 °C	−55 °C–85 °C	2 (on blue-green roof)	In soil under panel (3 cm depth)

2.3. Data analysis methods

The presented data are from the measurement period of June up until October 2022. To answer the research question, the performance in terms of solar PV output of both roofs should be compared. Yet, as discussed in the introduction, the PV output is influenced by panel temperature, which is subsequently influenced by air and/or roof temperature. To better understand the relationships between temperature and power output, we have done multiple analyses, and used methods that are commonly applied in similar research on green roofs with PV systems.

- 1. Data cleaning

We have only used daytime values (Irradiation >4 Wm^{-2}) and removed outliers of PV output. If the average energy output of 6 measured panels was higher than their maximum capacity (385 Wh) or the energy production was very low (<3 Wh) while the irradiation was >100 Wm^{-2}, the data were excluded from further analysis.

- 2. PV performance analysis

To determine the differences in PV performance under different weather conditions, the data were divided into bins of both temperatures (per 5 °C) as well as irradiation (per 100 Wm^{-2}), according to the same method as Nagengast et al. (2013) [18]. Due to differences in shading on both roofs in the early morning hours mostly during autumn and winter (Fig. 3), we have chosen to not compare the roofs at similar moments in time, but at similar irradiance. This was possible because we have placed two irradiance sensors at both roofs in the same area as the measured PV panels. Besides an orderly presentation of data, we performed a linear regression analysis (OLS method) on the daytime dataset for both roofs, to find a relationship between irradiance and solar PV output, with the intercept at 0 (at zero irradiation, there will be no PV output) and a 95% confidence interval, which is a common method in other research on green roofs with PV systems [8,15,18,27].

- 3. Multi-linear regression of PV performance with more parameters

To obtain more insights on the factors influencing solar panel performance, a correlation table was made followed by a multi-linear regression analysis for the most important parameters while avoiding collinearity. Similar methods have been applied in earlier research [13, 18]. In the combined dataset, all measurements from both roofs were merged, whereby roof type was added as a parameter (integer, BGR = 1, BiR = 0). A correlation table was obtained for the correlation values between PV performance and roof type, irradiation Irr, relative humidity RH, PV back panel temperature T_p, roof surface temperature T_S, air temperature under PV panel T_a, the ambient air temperature above the roof (1.25 m) T_{amb}, and wind (nearby Schiphol weather station).

- 4. Temperature analysis and estimation of sensible heatflux

Besides solar panel output, differences in temperature and sensible heatflux between both roofs provide valuable data as well for comparison and to further explore how differences in solar output can be explained. Therefore, both maximum as well as average differences in temperature of PV back panel temperature T_p, roof surface temperature T_S, air temperature under PV panel T_a, the ambient air temperature above the roof (1.25 m) T_{amb} were calculated. Segmented linear regression [28] was used to explore relationships between differences in T_S, T_a and T_p.

The sensible heat flux Q_H (Wm^{-2}) is proportional to the difference between surface temperature and air temperature measured at a certain level times a convective heat transfer coefficient [29]. Q_H was calculated according to:

$$Q_H = h_c \bullet (T_S - T_a) \quad \text{(Eq 2)}$$

With h_c the convective heat transfer coefficient ($W\ m^{-2}K^{-1}$). h_c can be approximated using the empirical Jürges formula which is used in urban canopy models [29–31]:

$$h_c = 5.9 + 4.1v \bullet \left(\frac{511 + 294}{511 + T_a}\right) \quad \text{(Eq 3)}$$

With v the wind velocity (ms^{-1}). Given the complexity of urban surfaces, it is questionable whether the application of an empirical heat transfer coefficient will provide exact values for Q_H. Xu & Asawa [31] mention an uncertainty of ±15–20% associated with the use of Jürges formula. Calculated values are, however, valuable for comparison between the two roofs and to other applications.

3. Results & discussion

3.1. PV performance

To assess the effect of roof type on PV performance, we present the average difference in PV power output and categorized the data based on both ambient temperature and solar irradiance. Overall, the BGR is constantly performing better than the BiR in all solar irradiance categories (see Table 4). The absolute difference is increasing as well, which is expected as the absolute solar output also increases with higher irradiance. A similar trend is seen for all temperature categories, although there is a significant outlier at the 5–10 °C/100–200 Wm^{-2} category (with only 1.2% of the data). The data thus suggest that for temperatures above 10 °C, regardless of the amount of irradiation, the PV system on the BGR produces more power than the BiR.

To quantify this effect further, we have done a linear regression analysis with all daytime data for both roofs with irradiation versus PV output. The 95% confidence interval is shown in Fig. 4, and the confidence intervals of both regression lines do not overlap, which means the difference in PV output between the two roofs is significant. Based on the regression values (see Table 5), the BGR roof would on average produce 4.4% more electrical energy at similar irradiance.

This result is on the higher side of the range based on available studies (see Table 1), for which we discuss two possible explanations. Firstly, different studies [20,21] pointed out that differences in enhanced solar panel performance between studies are influenced by the height of the panels above the roof. The higher the panels are placed, the larger the cooling effect of the airflow is. This could have influenced the almost insignificant results of Nagengast et al. [18] who conclude that only if the temperature is > 25 °C/irradiance >800 Wm^{-2} a green roof would make a difference on PV panel output, otherwise it would not. However, the height of the panels above the green roof was 53 cm, and for the black roof 13 cm, so this could explain the small difference. The study of Alshayeb & Chang [6] could have been influenced by the different heights as well. Here, the sedum is placed under already installed panels which results in less height between the surface and panel on a green roof than with a black surface. The same seems to be true for Schindler et al. [12], although the windy climate could have influenced the results here as well, combined with the low evaporation of plants on the green roof. Our study is one of the few studies with a long-term large-scale set-up that paid attention to comparable heights between PV systems on both roof types. Secondly, our BGR has a continuous water supply and capillary irrigation, and therefore as shown in Cirkel et al. (2018) [2] and Busker et al. (2022) [11] evapotranspiration will not decline due to water limitation during dry periods, as in other studies [12]. An inconvenience of our setup was the difference in shadow effects between the BGR and BiR. Therefore, the BGR is longer exposed to sunlight than the BiR, so even at similar irradiation, the BGR is already receiving sunlight for a longer period and thus the solar panels could already have warmed up slightly, this could have influenced our results. That means that our results could be on the conservative side, so with similar shadow effects, the BGR could possibly perform even better than measured here. Yet, these moments occur only at the beginning of the day with lower irradiation (<200 W/m^{-2} so the bottom left corner of the graph), when the effect is less significant due to low PV output, and where most data points are located (40.6%), thus a possible effect is damped. Furthermore, we know from the temperature data (see section 3.3, 3.4 & 3.5 for a further analysis) that the solar panels on the bitumen roof quickly warm up when receiving irradiation, thus the effect diminishes within about 1 h. Therefore, the influence on the results of the difference in shading on both roofs is minimal.

Table 4
Average difference in solar PV output of 6 panels on each roof presented as solar output BGR– solar output BiR in kW (kWh/hr) is shown. The data are categorized according to solar irradiance and ambient temperature. Table layout inspired by Nagengast et al. *(2013)* [18].

Solar Irradiance (Wm^{-2}) - Irr	Ambient temperature (°C) - T_{amb}										Weighted average BGR – BiR per panel (kW)	% of data
	< −5	-5–0	0–5	5–10	10–15	15–20	20–25	25–30	30–35	>35		
0–100				0.2	2.0	0.1	−0.7	−1.0			*0.6*	23.9
100–200				−6.3[a]	4.8	3.3	−0.8	−1.0			*1.7*	16.7
200–300					8.9	2.0	1.3	0.9	7.3[a]	−4.7[a]	*2.5*	14.0
300–400					14.5	4.8	6.8	−4.1	4.7[a]	−1.8[a]	*5.2*	11.9
400–500					−1.8	9.4	3.8	17.2	19.6[a]		*3.1*	11.1
500–600					6.7[a]	−0.7	11.2	6.4	15.1	10.4[a]	*6.1*	7.7
600–700					4.8[a]	16.7	9.8	2.1	19.0	5.6[a]	*6.1*	7.6
700–800						13.2	13.0	16.3	12.3[a]	−3.5[a]	*9.8*	4.9
800–900						19.0[a]	14.2	10.0			*9.0*	2.1
900–1000						8.1[a]					*4.1*[a]	0.1
>1000												
Weighted average BGR – BiR (kW)	*0*	*0.0*	*0.0*	*−1.1*	*4.6*	*5.5*	*6.0*	*5.6*	*13.6*	*1.2*		
% of Data	0	0.0	0.0	1.2	16.7	49.4	24.4	6.8	1.2	0.2		

[a] Value is based on 1–3 datapoints.

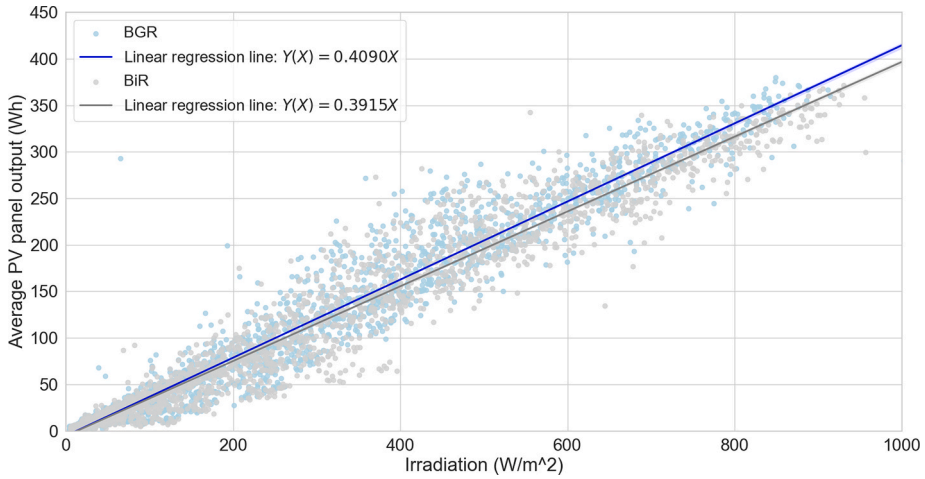

Fig. 4. Linear regression results including a 95% confidence interval for the average PV panel output versus irradiation in Wm^{-2} for both the BiR) and BiR based on all hourly daytime data, outliers removed.

Table 5
Linear regression results (OLS method) for irradiation vs PV panel output for both roof types.

	Number of observations	Coefficient (irradiation/PV panel output)	t-statistic	P-value	R^2
BiR	2048	0.3915	291.7	0.000	0.977
BGR	2048	0.4090	294.1	0.000	0.977

3.2. Multi-regression analysis

We have performed a multi-linear regression analysis on the combined dataset of the two roofs to determine if the roof type has a significant effect on the PV panel output, roof type was added to the dataset as a parameter (BGR = 1, BiR = 0).

Then the correlation coefficients of all measured parameters were analyzed (Table 6) to check which parameters influence each other. The roof type has only a small negative correlation with T_S, meaning that the BGR tends to result in a lower roof surface temperature. On the other parameters, no effect is visible, which means as well that there is no risk of multicollinearity with other parameters. Moreover, we see that T_S and T_{amb} are highly correlated and thus should not both be included in the multilinear regression equation. The same line of reasoning is valid for the T_S and T_p, and for T_{amb} and T_p. Therefore, we have chosen to include the air temperature T_{amb}, and not T_S and T_p in the regression analysis. Furthermore, irradiance (*Irr*) was included as we know it highly affects PV output. To assess the effect of roof type, two analyses were done.

First, we have taken only the irradiation and air temperature into account and evaluated how these two parameters explain the variance PV power output. With an $R^2 = 0.943$ the coefficients were significant ($P < 0.05$) at a 95% confidence interval (Table 7). Secondly, we have added the roof type as a factor in the regression analysis. The roof type proves to be significant as well ($P < 0.05$) and the R^2 for the combined analysis of irradiation, solar panel temperature and roof type was 0.944 (Table 8). Thus, the roof type proves to be a significant factor, although it does not explain the variance in the data significantly more than without the roof type included as a factor.

Table 6
Correlation coefficients for roof type (here interpreted as BG = 1), air temperature above the roof (T_{air}), irradiation (Irr), relative humidity (RH), PV panel back temperature (T_p), roof surface temperature under the panel (T_S) and air temperature under a PV panel ($T_{a,p}$) for the combined dataset of the two roofs (day values).

	Roof type	T_{amb}	Irr	RH	T_p	T_S	T_a
Roof type (1 is BG, 0 is BiR)	1						
T_{amb}	−0.02	1					
Irr	−0.03	0.47	1				
RH	0.02	−0.74	−0.65	1			
T_p	−0.02	0.79	0.87	−0.78	1		
T_S	−0.21	0.90	0.61	−0.76	0.87	1	
T_a	−0.03	0.99	0.53	−0.76	0.84	0.93	1

3.3. Differences in surface temperature T_S, Air temperature below panels T_a and back of panel temperature T_p

The daytime roof surface temperature T_S measured underneath the PV panels was lower on the BGR compared to the BiR. ΔT_S (BiR – BGR) increases with higher irradiation and can become as high as 12 °C on a clear summer day (Fig. 5). Mean daytime T_S were lower on the blue-green roof with a statistically significant difference of 2.39 °C. Although less pronounced, the BiR indicates a measurable, positive effect on the daytime near-roof air temperature T_a measured below the PV panels. During the measurement period, T_a was on average 0.19 °C higher on the BiR, this difference was however statistically non-significant. A maximum ΔT_a of 2.63 °C was reached on August 14, 2022 at 14:00 p.m. Mean T_p was almost equal on the BiR and BGR (mean $\Delta T_p = -0.05$). There were several periods where positive ΔT_p's were measured, reaching a maximum ΔT_p of 6.63 °C on September 2, 2022.

However, as is also visible in Fig. 5, there are negative spikes in the ΔT_S, ΔT_a and especially ΔT_p data, indicating a higher T_p on the BGR compared to the BiR. This is caused by shade from a nearby tall building on the BiR in the morning before 11 a.m. (Fig. 3). Even with the sun at its highest azimuth (around the 21st of June) we still see these shadow effects causing discrepancies in the amount of irradiance on both roofs, resulting in lower temperatures on the BiR. Besides these shading effects, there are also periods with negative ΔT_p, ΔT_a (Fig. 5) and

Table 7
Multi-regression analysis results for PV panel output variance explained by air temperature and irradiation.

	Coefficient	Standard Deviation	t-statistic	P-value
Intercept	4.86	1.665	2.93	0.003
Irr	0.415	0.002	237	0.000
T_{air}	−0.599	0.096	−6.25	0.000
R^2		0.943		
No. of observations		4210		

Table 8
Multi-regression analysis results for PV panel output variance explained by air temperature, irradiation and roof type.

	Coefficient	Standard Deviation	t-statistic	P-value
Intercept	1.943	1.69	1.15	0.25
Irr	0.415	0.002	237	0.000
T_{air}	−0.598	0.095	−6.27	0.000
Roof type	5.50	0.74	7.44	0.000
R^2		0.944		
No. of observations		4210		

sometimes even negative ΔT_S. So, although the mean surface temperature of the BGR is significantly cooler than the BiR and we saw in Fig. 5 that there seemed to be a smaller but similar effect on ΔT_a as well as ΔT_p, there are also periods where temperatures measured at the BiR are lower than at the BGR.

3.4. Differences in estimated sensible heat flux

Sensible heat flux estimates Q_H, below the PV panels, were higher at the BiR compared to the BGR with a significant mean difference of 52.5 W m^{-2}. During our measuring period estimated Q_H at the BGR stayed below 60.0 W m^{-2} and were often very small, or even negative during daytime (Fig. 6). At the BiR estimated Q_H was much higher with a mean value of 50.2 W m^{-2} and peaks reaching 291.1 W m^{-2}. Negative sensible heat flux estimates point to a so-called oasis effect, where energy is transferred from the surrounding air to the plants and used for evapotranspiration. The observed negative daytime Q_H estimates on the BGR coincide with cooler T_a and T_p on the BGR (Fig. 5). Note that the above Q_H estimates are based on temperature measurements in the shade of PV panels, resulting in relatively low sensible heat flux densities. In literature values for Q_H reaching up to 280 and 750 W m^{-2} were found for respectively green and bitumen roofs without the shade of PV panels in a similar climatic setting [29].

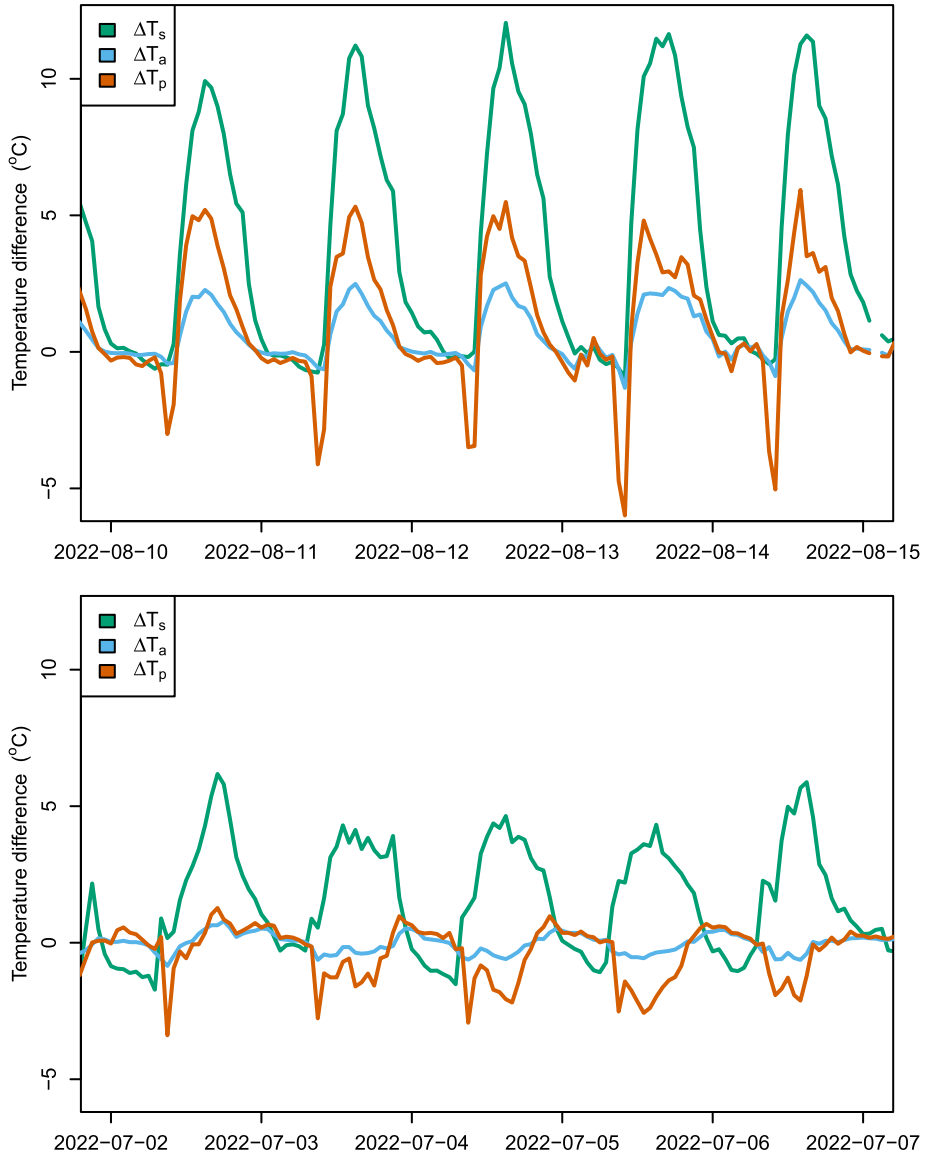

Fig. 5. Hourly differences in temperature (ΔT_s, ΔT_a and ΔT_p) between the BiR and the BGR during the periods 10–15 August and 2–7 July. A positive value means that the temperature measured at the bitumen roof is higher than at the blue-green roof. (For interpretation of the references to colour in this figure legend, the reader is referred to the Web version of this article.)

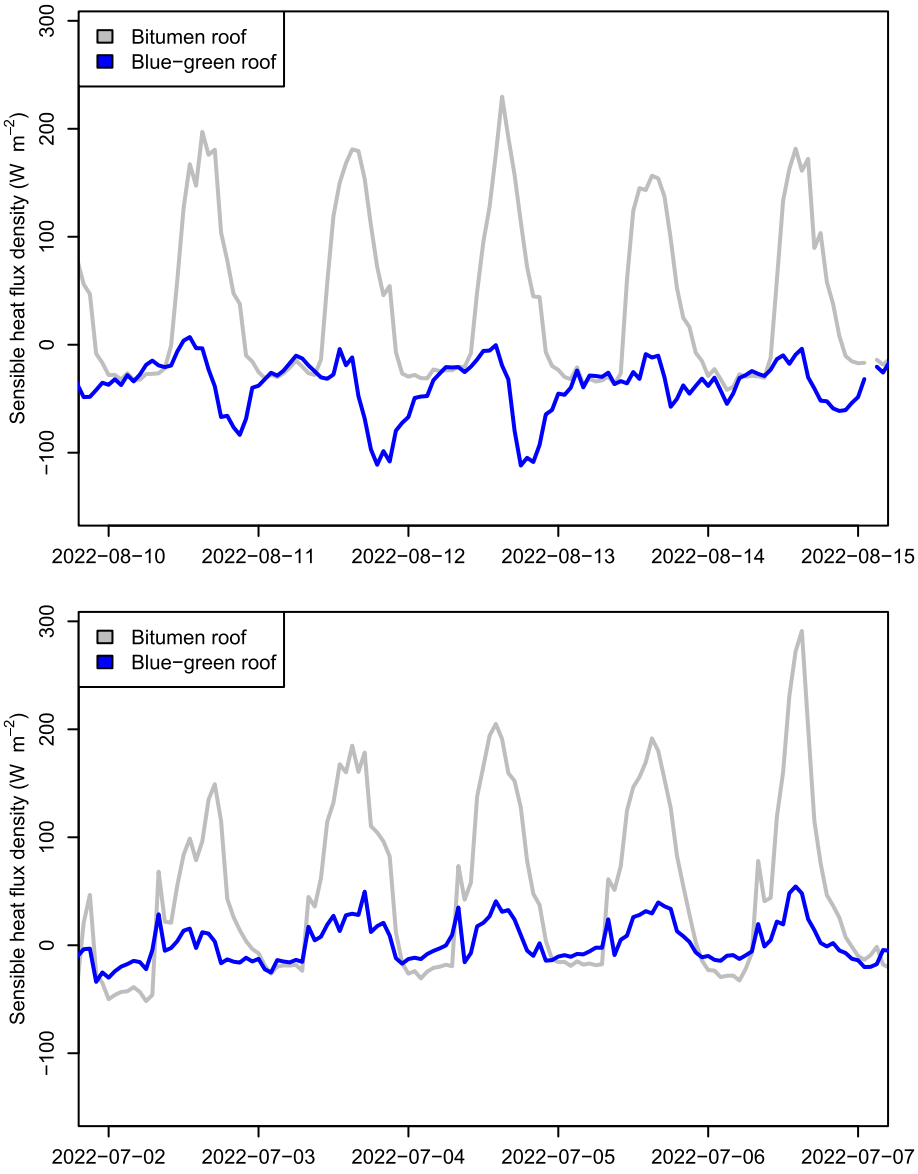

Fig. 6. Estimated sensible heat flux densities Q_H on both roofs for two periods: 10–15 August and 2–7 July.

3.5. Nonlinear relation between T_s, T_a and T_p

From earlier studies, we know that a clear temperature effect of green-solar roofs [6,8] versus bitumen roofs is expected. There are several explanations for our more ambiguous results. On the BGR energy is stored in the substrate and water storage layer, buffering temperature fluctuations at the surface. As a result, the cooling rate of the bitumen roof is higher over the course of the night resulting in lower nocturnal T_S than the green roof [29]. Note that in our setup T_S is measured in the shade of the solar panels on both roofs, which delays the warming effect of irradiation in the morning. Another explanation can be found in rainfall. After rainfall events, not all rainfall is drained from the BiR immediately and the roof surface stays wet for several hours or even days until the remaining water is evaporated, cooling down the BiR surface during that process. Wind effects can also play a role, mainly in the sense that the cooling effect of wind can overrule the effects of roof temperature. For example, Osma-Pinto & Ordóñez-Plata [14] conclude that the air velocity is more influential than the roof type, at least in warm and tropical climates. Lastly, positive effects of the BGR besides the roof temperature could be the difference in albedo between both roofs [32].

Additional analysis was done to further understand the temperature effects. We found that there is a significant positive non-linear relationship between ΔT_s and ΔT_a (R^2: 0.69) and between ΔT_s and ΔT_p (R^2: 0.43) (Fig. 7). Fitting segmented linear regression models [28] on the data results in two linear sections with different slopes for each relation with an estimated significant breakpoint at $\Delta T_s = 4.64$ °C (st. err. 0.14 and 0.31). Below this temperature difference there is almost no measurable relation between ΔT_s and ΔT_a or ΔT_p. The cooling effect of the BGR thus has to result in an at least 4.64 °C lower surface temperature compared to the BiR, before an effect on ΔT_a *and* T_p becomes measurable.

3.6. Reflection on vegetation-PV feedback and interaction

Our results confirm that vegetation has a positive influence on PV performance. From the literature we know there is also an effect of PV on the vegetation; PV systems on green roofs lead to lower evapotranspiration due to the shade effect of the PV panels [27]. In warm climates, the shading of the PV panels can even lead to faster growth of vegetation and 50% lower pigment levels [14]. The type of plant chosen also affects the power output performance [21]. During our measurements,

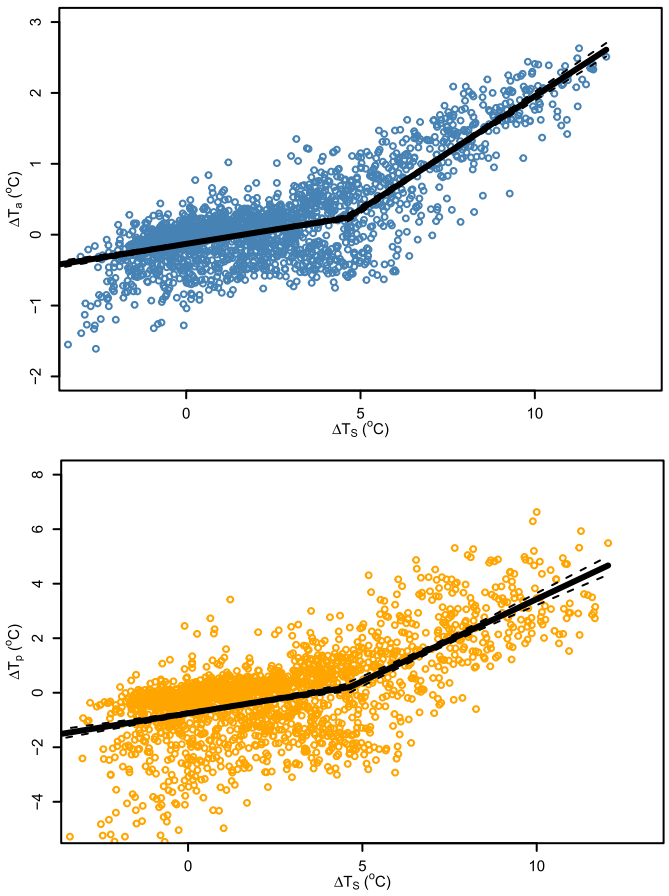

Fig. 7. Relation between ΔTs and ΔTa and ΔTs and ΔTp and fitted segmented linear regression lines with 95% confidence intervals.

relatively low sedum species still dominated the vegetation, but (taller) native herbs started to slowly overtake the vegetation and gradients in plant growth became visible between shaded and sunny areas (Fig. 8). Below the panels, plants remained relatively low. In the sunny paths between the panel rows plant growth was more abundant. If succession proceeds to a grass/herbs-dominated vegetation with taller plants, this might also affect air circulation underneath the PV panels. As we discussed in the previous section air velocity can be an important factor in cooling PV panels [14]. Taller vegetation might therefore result in a less positive effect on PV output than observed during our measurement period. Lysimeters and more detailed wind and radiation measurements are needed to further investigate the effects of the solar panels and plant development on wind effects, actual evaporation and energy fluxes. Moreover, fault detection algorithms [33] could possibly assist in the online monitoring of the plant height and potential influence on PV output to know when maintenance of the vegetation would be necessary. On the other hand, algorithms developed for the optimal planning and packing of rooftop PV systems [34,35] could be extended to include the possibility of (blue)-green roofs as well.

3.7. Considerations on energy use of the grey water system

The grey water system in the building provided a more continuous water supply for the vegetation and therefore prevented drought stress. As a result, transpiration and the cooling effect of the plants can be considered optimal for the meteorological conditions during the measurement period. However, the abundant supply of water comes at a price. Energy is needed to pump the collected shower water from the basement to the roof. We have calculated that the (multi-05) pump which has to overcome 34 m of height difference can pump about 1 m^3 per hour at full capacity (900 W). Depending on if the water supply to the roof is only functioning during spring and summer, or during the whole year, this means that between 65 and 160 kWh per year is needed for pumping. The expected extra production of the BGR versus the BiR with 62 panels is about 970 kWh/year (405 Wp panels, based on the 4.4% higher power production). Thus, 7–17% of the expected extra power production is needed for the water supply on the roof, which is significant, yet manageable. Moreover, the water supply is not only influencing (indirectly) the solar panel output, but is used for the vegetation on the balconies and lower roofs as well. Overall, the extra solar power output is expected to more than compensate the pump energy, the water system meanwhile is also enhancing other positive effects of the building such as reducing heat stress, increased urban plant coverage, increased biodiversity and better stormwater management [16,21].

3.8. Implications for water- and energy-sensitive buildings

The design and construction of the twin buildings, where we performed our research, required a lot of extra effort from all parties involved because of the non-conventional water system in the building and multifunctional use of the rooftops for energy, vegetation and water management. The most important lessons learned are:

- Sustainability goals like water circularity, stormwater management, biodiversity, energy production and improved liveability for the tenants have to be considered and included in the designs from the start of the process because these goals affect architecture, structural design, rooftop waterproofing systems and water- and power infrastructure from the basement all the way up to the roof.
- Where in the past the roof was considered lost space where for example HVAC, ventilation and other technical infrastructure could be placed where convenient, with the multifunctional approach it now becomes important to minimise the amount of space used for

Fig. 8. Impression of the vegetation in between the PV panels (sunnier area) and under the PV panels (shaded area).

this infrastructure and cluster it in limited and specific areas on the roof.

- Normally the roof is the 'final' stage of waterproofing the building, yet to create a multifunctional rooftop landscape, specialists from different fields (ventilation and HVAC, power, water management, landscaping, solar PV) should be involved in design and construction. This requires understanding, extra cooperation and design, and smart building planning between these specialists, to construct the roof in an efficient manner.
- When creating buildings with novel and innovative water management systems, it will take at least one year after construction (covering all seasons) to optimise the systems and get experience in actual required maintenance to be incorporated in the final maintenance manual. Clearly appoint responsibility and budget time and money for these tasks.

4. Conclusion

We have investigated the performance of a full-scale solar PV system on a bitumen roof and a blue-green capillary irrigated roof on twin buildings in Amsterdam. Based on a 5-month data collection period (June–October 2022) we see a clear positive effect of the BGR on the PV performance. On average, a solar panel on the BGR is expected to produce 4.4% more energy than a solar panel on the BiR at similar irradiation, in a North-West European climate. The positive effect is seen at air temperatures above 10 °C, regardless of irradiation. A clear difference in panel temperature on the roofs is only seen when the surface temperature of the roofs differs by at least 4.64 °C. Otherwise, other factors such as wind or albedo have probably more influence on the PV panel temperature and thus on PV power output. Overall, we have shown that a blue-green PV roof creates a win-win-win situation both for PV production, the local water balance as well as biodiversity. Future research could better investigate wind and albedo effects, different heights of solar panels above the roof and development of the vegetation and the effects of this changing vegetation on PV output.

Funding

This publication is a result of the TKI project Urban Photosynthesis and is co-financed with PPS funding from the Topconsortia for Knowledge & Innovation (TKI's) of the Ministry of Economic Affairs and Climate, the Netherlands.

Data

The dataset of the sensors and PV output of the measured panels on both roofs that was used for this publication can be accessed via https://doi.org/10.4121/679c03a2-bcae-46b9-a4f0-91c230708ca5.v1.

CRediT authorship contribution statement

Els van der Roest: Writing – review & editing, Writing – original draft, Visualization, Methodology, Investigation, Funding acquisition, Formal analysis, Data curation, Conceptualization. **Joris G.W.F. Voeten:** Writing – review & editing, Visualization, Investigation, Funding acquisition, Conceptualization. **Dirk Gijsbert Cirkel:** Writing – review & editing, Writing – original draft, Visualization, Validation, Project administration, Methodology, Investigation, Funding acquisition, Formal analysis, Data curation, Conceptualization.

Declaration of competing interest

The authors declare the following financial interests/personal relationships which may be considered as potential competing interests: Co-author Joris Voeten has been previously employed by Permavoid B.V. until 30th of June 2021.

Acknowledgements

We would like to thank Aedes Care BV/Plan 8 Vastgoedontwikkeling BV for facilitating this research by making it possible to perform this full-scale research on their water-sensitive and green building and facilitating the research in all possible ways. We furthermore thank the technical project partners for the fruitful collaboration and technical base underneath the project: Permavoid B.V., ECOFYT, Techniplan Adviseurs BV, and SDR Elektrotechniek BV. We would like to thank Solnet for letting us monitor the solar panels and install sensors on them.

Also, we thank the municipality of Amsterdam for their cooperation on the research concerning the tenants and the outreach/communication. Lastly, Pim Post and Diederik van Hasselt (deceased) are thanked for their help with the statistical analysis.

References

[1] A. Scherba, D.J. Sailor, T.N. Rosenstiel, C.C. Wamser, Modeling impacts of roof reflectivity, integrated photovoltaic panels and green roof systems on sensible heat flux into the urban environment, Build. Environ. 46 (12) (2011) 2542–2551, https://doi.org/10.1016/j.buildenv.2011.06.012, 10.1016/j.buildenv.2011.06.012. [Online]. Available:.

[2] D.G. Cirkel, B.R. Voortman, T. van Veen, R.P. Bartholomeus, Evaporation from (Blue-)Green roofs: assessing the benefits of a storage and capillary irrigation system based on measurements and modeling, Water 10 (9) (Sep. 2018) 1253, https://doi.org/10.3390/w10091253 [Online]. Available: http://www.mdpi.com/2073-4441/10/9/1253.

[3] D.B. Rowe, K.L. Getter, The role of extensive green roofs in sustainable development, Hortscience 41 (5) (2006) 1276–1285.

[4] M. Shafique, R. Kim, M. Rafiq, Green roof benefits, opportunities and challenges – a review, Renew. Sustain. Energy Rev. 90 (April) (2018) 757–773, https://doi.org/10.1016/j.rser.2018.04.006.

[5] B.R. Paudyal, A.G. Imenes, Investigation of temperature coefficients of PV modules through field measured data, February, Sol. Energy 224 (2021) 425–439, https://doi.org/10.1016/j.solener.2021.06.013, 10.1016/j.solener.2021.06.013. [Online]. Available:.

[6] M. Alshayeb, J. Chang, Variations of PV panel performance installed over a vegetated roof and a conventional black roof, Energies 11 (5) (May 2018) 1110, https://doi.org/10.3390/en11051110 [Online]. Available: http://www.mdpi.com/1996-1073/11/5/1110.

[7] R. Ciriminna, F. Meneguzzo, M. Pecoraino, M. Pagliaro, Solar green roofs: a unified outlook 20 Years on, Energy Technol. 7 (6) (2019) 1–7, https://doi.org/10.1002/ente.201900128.

[8] H.H.K. Ogaili, Measuring the Effect of Vegetated Roofs on the Performance of Photovoltaic Panels in Combined Systems, Portland University, 2015 [Online]. Available: https://pdfs.semanticscholar.org/5dcf/fec3a8c3a99179ab934cb4569182d3885095.pdf.

[9] C. Catalano, N. Baumann, Biosolar roofs: a symbiosis between biodiverse green roofs and renewable energy, City Green 15 (2017) 42–49 [Online]. Available: https://www.nparks.gov.sg/-/media/cuge/ebook/citygreen/cg15/cg15_05.pdf?la=en&hash=742D039957FCA9CB7640F52498428F81CAAF42A9.

[10] M. Shafique, R. Kim, D. Lee, The potential of green-blue roof to manage storm water in urban areas, Nat. Environ. Pollut. Technol. 15 (2) (2016) 715–718.

[11] T. Busker, et al., Blue-green roofs with forecast-based operation to reduce the impact of weather extremes, June 2021, J. Environ. Manag. 301 (2022), 113750, https://doi.org/10.1016/j.jenvman.2021.113750, 10.1016/j.jenvman.2021.113750. [Online]. Available:.

[12] B.Y. Schindler, L. Blaustein, R. Lotan, H. Shalom, G.J. Kadas, Green roof and photovoltaic panel integration : effects on plant and arthropod diversity and electricity production, March, J. Environ. Manag. 225 (2018) 288–299, https://doi.org/10.1016/j.jenvman.2018.08.017, 10.1016/j.jenvman.2018.08.017. [Online]. Available:.

[13] D. El Helow, Performance of Green Roof Integrated Solar Photovoltaics in Toronto, University of Toronto, 2018. Online]. Available: https://hdl.handle.net/1807/89540.

[14] G. Osma-Pinto, G. Ordóñez-Plata, Measuring factors influencing performance of rooftop PV panels in warm tropical climates, Sol. Energy 185 (April) (2019) 112–123, https://doi.org/10.1016/j.solener.2019.04.053, 10.1016/j.solener.2019.04.053. [Online]. Available:.

[15] M.J.R. Perez, N.T. Wight, V.M. Fthenakis, C. Ho, Green-roof integrated pv canopies-an empirical study and teaching tool for low income students in the South Bronx, World Renew. Energy Forum, WREF 2012, Incl. World Renew. Energy Congr. XII Color. Renew. Energy Soc. Annu. Conf. 5 (1) (2012) 4046–4052.

[16] D. Chemisana, C. Lamnatou, Photovoltaic-green roofs : an experimental evaluation of system performance, Appl. Energy 119 (2014) 246–256, https://doi.org/10.1016/j.apenergy.2013.12.027, 10.1016/j.apenergy.2013.12.027. [Online]. Available:.

[17] M. Köhler, W. Wiartalla, R. Feige, Interaction between PV-systems and extensive green roofs, in: Greening Rooftops for Sustainable Communities, 2007, pp. 1–16 [Online]. Available: http://www.worldgreenroof.org/files/pdf/Manfred-KoehlerMinneapolisPV.pdf.

[18] A. Nagengast, C. Hendrickson, H. Scott Matthews, H.S. Matthews, Variations in photovoltaic performance due to climate and low-slope roof choice, Energy Build. 64 (2013) 493–502, https://doi.org/10.1016/j.enbuild.2013.05.009, 10.1016/j.enbuild.2013.05.009. [Online]. Available:.

[19] H. Alameddine, L. Sharman, P. Irga, R. Fleck, F. Torpy, E. Wooster, Green Roof & Solar Array-Comparative Research Project, 2021 [Online]. Available: https://opus.lib.uts.edu.au/handle/10453/150142.

[20] H. Ogaili, D.J. Sailor, Measuring the effect of vegetated roofs on the performance of photovoltaic panels in a combined system, J. Sol. Energy Eng. 138 (6) (Dec. 2016) 1–8, https://doi.org/10.1115/1.4034743 [Online]. Available: https://asmedigitalcollection.asme.org/solarenergyengineering/article/doi/10.1115/1.4034743/380622/Measuring-the-Effect-of-Vegetated-Roofs-on-the.

[21] M. Shafique, X. Luo, J. Zuo, Photovoltaic-green roofs: a review of benefits, limitations, and trends, October 2019, Sol. Energy 202 (2020) 485–497, https://doi.org/10.1016/j.solener.2020.02.101, 10.1016/j.solener.2020.02.101. [Online]. Available:.

[22] M. Zapater-Pereyra, S. Lavrnić, F. van Dien, J.J.A. van Bruggen, P.N.L. Lens, Constructed wetroofs: a novel approach for the treatment and reuse of domestic wastewater, Ecol. Eng. 94 (2016) 545–554, https://doi.org/10.1016/j.ecoleng.2016.05.052.

[23] G. Osma, G. Ordóñez, E. Hernández, L. Quintero, M. Torres, The impact of height installation on the performance of PV panels integrated into a green roof in tropical conditions, in: Energy Production and Management in the 21st Century II: the Quest for Sustainable Energy, vol. 1, 2016, pp. 147–156, https://doi.org/10.2495/eq160141.

[24] D. El Helow, J. Drake, L. Margolis, Testing the potential synergy of green roof-integrated photovoltaics at the university of Toronto green roof innovation testing (GRIT) laboratory, 32nd RCI International Convention and Trade Show no. August (2017) 229–235.

[25] G.F. Makkink, Testing the penman formula by means of lysimeters, J. Inst. Water Eng. 11 (1957) 277–288.

[26] J. G. W. F. Voeten, L. van de Werken, and A. P. Newman, "Demonstrating the Use of Below-Substrate Water Storage as a Means of Maintaining Green Roofs -Performance Data and a Novel Approach to Achieve Public Understanding," *World Environmental and Water Resources Congress*. ASCE Library, West Palm Beach, FL, USA, pp. 12–21, Feb. 02, 2016 [Online]. Available: https://doi.org/10.1061/9780784479841.002.

[27] A. Jahanfar, J. Drake, B. Gharabaghi, B. Sleep, An experimental and modeling study of evapotranspiration from integrated green roof photovoltaic systems, July 2019, Ecol. Eng. 152 (2020), 105767, https://doi.org/10.1016/j.ecoleng.2020.105767, 10.1016/j.ecoleng.2020.105767. [Online]. Available:.

[28] V.M.R. Muggeo, segmented: an R Package to fit regression models with broken-line relationships, R. News 8 (1) (2008) 20–25 [Online]. Available: https://journal.r-project.org/articles/RN-2008-004/RN-2008-004.pdf.

[29] J. Heusinger, S. Weber, Comparative microclimate and dewfall measurements at an urban green roof versus bitumen roof, Build. Environ. 92 (2015) 713–723, https://doi.org/10.1016/j.buildenv.2015.06.002, 10.1016/j.buildenv.2015.06.002. [Online]. Available:.

[30] F. Chen, et al., The integrated WRF/urban modelling system: development, evaluation, and applications to urban environmental problems, Int. J. Climatol. 31 (2) (2011) 273–288, https://doi.org/10.1002/joc.2158.

[31] X. Xu, T. Asawa, Systematic numerical study on the effect of thermal properties of building surface on its temperature and sensible heat flux, Build. Environ. 168 (October 2019) 2020, https://doi.org/10.1016/j.buildenv.2019.106485.

[32] M.P. Brennan, A.L. Abrahamse, R.W. Andrews, J.M. Pearce, Effects of spectral albedo on solar photovoltaic devices, Sol. Energy Mater. Sol. Cells 124 (2014) 111–116, https://doi.org/10.1016/j.solmat.2014.01.046, 10.1016/j.solmat.2014.01.046. [Online]. Available:.

[33] E.A. Sarquis Filho, et al., Practical recommendations for the design of automatic fault detection algorithms based on experiments with field monitoring data, Sol. Energy 244 (August) (2022) 227–241, https://doi.org/10.1016/j.solener.2022.08.022, 10.1016/j.solener.2022.08.022. [Online]. Available:.

[34] S. Jung, J. Jeoung, H. Kang, T. Hong, Optimal planning of a rooftop PV system using GIS-based reinforcement learning, June, Appl. Energy 298 (2021), 117239, https://doi.org/10.1016/j.apenergy.2021.117239, 10.1016/j.apenergy.2021.117239. [Online]. Available:.

[35] H. Ren, Y. Sun, C.F. Norman Tse, C. Fan, Optimal packing and planning for large-scale distributed rooftop photovoltaic systems under complex shading effects and rooftop availabilities, March, Energy 274 (2023), 127280, https://doi.org/10.1016/j.energy.2023.127280, 10.1016/j.energy.2023.127280. [Online]. Available:.